

# Hard X-ray multilayer zone plate with 25-nm outermost zone width

**H Takano<sup>1,5</sup>, K Sumida<sup>1</sup>, H Hiroto<sup>1,6</sup>, T Koyama<sup>2</sup>, S Ichimaru<sup>3</sup>, T Ohchi<sup>3</sup>, H Takenaka<sup>4</sup> and Y Kagoshima<sup>1,\*</sup>**

<sup>1</sup> Graduate School of Material Science, University of Hyogo, 3-2-1 Kouto, Kamigori, Ako, Hyogo 678-1297, Japan

<sup>2</sup> JASRI/SPring-8, 1-1-1 Kouto, Sayo, Hyogo 679-5198, Japan

<sup>3</sup> NTT Advanced Technology Corporation, 3-1 Morinosato, Wakamiya, Atsugi, Kanagawa 243-0124, Japan

<sup>4</sup> TOYAMA Co., Ltd., 3816-1, Kishi, Yamakita, Ashigarakami, Kanagawa 258-0112, Japan

\*E-mail: kagosima@sci.u-hyogo.ac.jp

**Abstract.** We have improved the performance of a previously reported multilayer zone plate by reducing its outermost zone width, using the same multilayer materials (MoSi<sub>2</sub> and Si) and fabrication technique. The focusing performance was evaluated at the BL24XU of SPring-8 using 20-keV X-rays. The line spread function (LSF) in the focal plane was measured using a dark-field knife-edge scan method, and the point spread function was obtained from the LSF through a tomographic reconstruction principle. The spatial resolution was estimated to be 30 nm, which is in relatively good agreement with the calculated diffraction-limited value of 25 nm, while the measured diffraction efficiency of the +1st order was 24%.

## 1. Introduction

X-ray microscopy is a powerful analytical tool for nondestructive observation of the internal structure of an object with high spatial resolution. Recently, X-ray focusing devices such as Fresnel zone plates (FZPs) and Kirkpatrick–Baez mirrors have achieved focused beam sizes of around 10 nm, becoming key technologies in X-ray microscopy [1-5]. An FZP is a circular transmission diffraction grating consisting of alternate transparent and opaque zones. Its spatial resolution  $\delta$  is determined by the outermost zone width ( $\Delta r_N$ ), namely  $\delta = 1.22\Delta r_N$ , where  $N$  is the total number of zones. Hence, the narrower the width  $\Delta r_N$ , the better the spatial resolution that can be achieved. On the other hand, diffraction efficiency is primarily determined by the thickness  $T$  of the zones in the X-ray propagation direction. In the hard X-ray region and for the zone materials generally used, the optimal thickness is greater than a few microns. Therefore, in that region, the zone structure should have an extremely high aspect ratio  $T/\Delta r_N$  (much larger than 100) to achieve high efficiency. However, zone structures with

<sup>5</sup> Present affiliation: Institute of Multidisciplinary Research for Advanced Materials, Tohoku University

<sup>6</sup> Present affiliation: SPring-8 Service Co., Ltd.



such high aspect ratios cannot currently be realized by electron beam lithography, which is the most frequently employed technique for FZP fabrication. To overcome this problem, multilayer zone plates (MZPs) were first proposed by Rudolph *et al.* [6] and subsequently investigated by several groups. An MZP is fabricated by stacking alternate layers on a cylindrical wire-like substrate and reducing the cross-section of the layers to an optimal thickness. It should be mentioned that there have been some outstanding works achieving sub-5 nm [7] and sub-30 nm spatial resolution [8].

We also developed an MZP fabrication technique and continued upgrading its optical performance [9–11]. A MoSi<sub>2</sub>/Si multilayer system was chosen for the MZP because of its superior heat resistance and diffusion at the interface [12]. The multilayer pairs were deposited on a glass fiber using magnetron sputtering, and the diameter of the fiber was measured by a laser scanner before the multilayer deposition. Multilayer thicknesses were designed based on the measured fiber diameter. The sectioning, polishing, and thinning of the MZP was done mechanically.

The most important performance parameter of an MZP as an optical device is its spatial resolution  $\delta$  and, as mentioned above, it is determined by the outermost zone width  $\Delta r_N$ . In our previous works, we attained increasingly narrower values of  $\Delta r_N$  (40 nm in [9, 10] and 30 nm in [11] and confirmed that a near diffraction-limited spatial resolution was attained. According to results calculated using coupled wave theory [13, 14], the local maximum diffraction efficiency as a function of  $\Delta r$  (the local grating half-pitch) starts to gradually decrease below  $\sim 30$  nm for a fixed photon energy of 20 keV [15]. Thus, we have almost reached a spatial resolution limit in the case of the present cylindrical flat layer MZP structure, where neither a tilted, nor a wedged, nor a curved-type multilayer structure [16] is adopted. However, values of  $\Delta r$  below 30 nm may still yield a practical diffraction efficiency. In this paper, we report the focusing performance of our upgraded MZP with  $\Delta r_N = 25$  nm using 20-keV X-rays.

## 2. Design parameters

A second important performance parameter for practical uses is the diffraction efficiency. It primarily depends on the zone thickness  $T$  because an MZP works as a phase zone plate under the assumption that the zone width  $\Delta r$  is sufficiently large to neglect dynamical diffraction effects. However, as  $\Delta r$  becomes smaller than  $\sim 30$  nm, less X-rays propagate through the zones due to dynamical diffraction effects, which leads to a decrease in the diffraction efficiency. Figure 1(a) shows the maximum local diffraction efficiency of diffraction gratings consisting of the same multilayer material (MoSi<sub>2</sub> and Si) as a function of the pitch for 20-keV X-rays, which was calculated by using coupled wave theory [13, 14]. In this calculation,  $T$  was chosen in order to maximize the diffraction efficiency for each value of

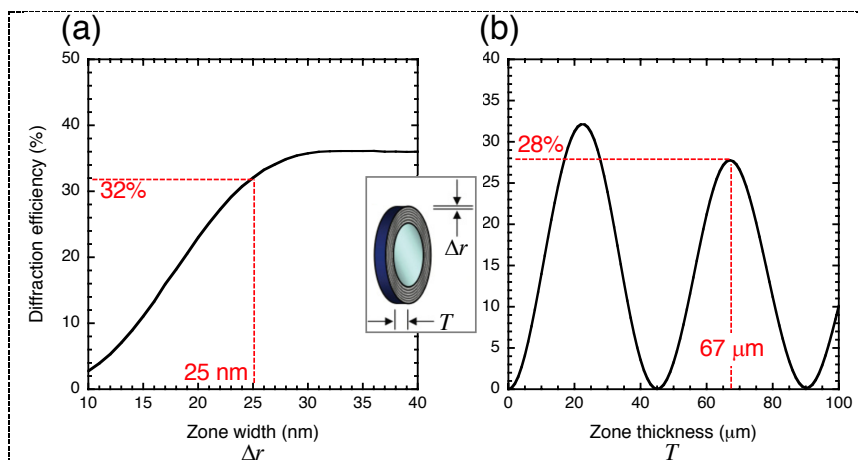


**Figure 1.** Maximum diffraction efficiency for a photon energy of 20 keV (calculated using coupled wave theory) as a function of (a) the grating half-pitch  $\Delta r$  and (b) the zone thickness  $T$  for  $\Delta r = 25$  nm.

the grating pitch  $2\Delta r$ . A zone width  $\Delta r$  of 25 nm yields a diffraction efficiency of 32%, which is not so low as compared to the maximum value of 36.1%. Figure 1(b) shows the diffraction efficiency as a function of  $T$ . The thickness that produces the maximum diffraction efficiency is 22  $\mu\text{m}$ , which is too small for the mechanical thinning. For this reason, we chose the second best diffraction efficiency of 28%, which occurs for  $T = 67 \mu\text{m}$ . The core of the MZP was a glass fiber, whose roundness was measured with a laser scanner (KEYENCE LS-7000). The fiber was rotated at  $5^\circ$  intervals, and for each angle, we measured the diameter at three points separated 5 mm and calculated the average. Taking again the average of all these average values, we obtained a fiber diameter of  $50.99 \pm 0.04 \mu\text{m}$ . The design parameters for this new MZP are shown in Table 1. Figure 2 shows the scanning electron microscopy (SEM) images of the fabricated MZP.

**Table 1.** Design parameters.

Layer material	MoSi <sub>2</sub> /Si
Outermost zone width $\Delta r_N$	25.2 nm
Total number of zones $N$	178
Diameter $D$	60.4 $\mu\text{m}$
Zone thickness $T$	67 $\mu\text{m}$
Focal length $f$	24.5 mm (at 20 keV)

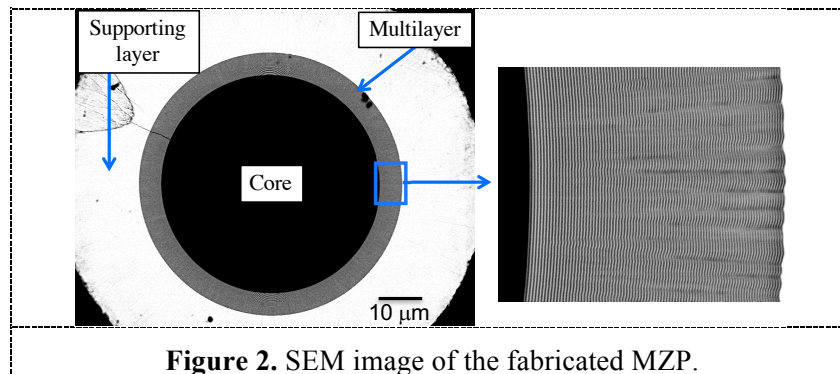


**Figure 2.** SEM image of the fabricated MZP.

### 3. Focusing performance

The line spread function (LSF) in the focal plane was measured at the BL24XU of SPring-8 using 20-keV X-rays. The optical system was the same as in [9]. Owing to the narrow annular aperture, subsidiary maxima of the point spread function (PSF) become much more intense than in the case of a circular aperture. As a result, the full-width at half-maximum (FWHM) of the LSF necessarily becomes much wider than FWHM of the PSF because an LSF convolutes the subsidiary maxima of the PSF. The calculated and measured LSFs are shown in Figure 3(a), where the latter was obtained using a dark-field knife-edge scan method [17]. The period of the ripples in the measured LSF is in good correspondence with that in the ideal LSF, although the base intensity is roughly two times higher. These oscillating structures come from the subsidiary maxima of the Airy pattern produced in the focal plane. The high base intensity may be caused by waviness of the outer zone layers. The distance between the first minima is 39 nm, which is in relatively good agreement with the diffraction-limited value of 36 nm. In order to evaluate the spatial resolution, one should not use the LSF but the PSF. In order to obtain the PSF from the measured LSF, we introduced a tomographic reconstruction principle [9, 10]. A single experimental LSF profile (dots in Figure 3(a)) was used as the representative LSF for the tomographic reconstruction. The half-distance between the first minima of the experimental PSF was estimated to be 30 nm, as shown in Figure 3(b). As the corresponding distance in the theoretical

PSF was 25 nm, we can conclude that near diffraction-limited performance was achieved by the MZP. Further, the measured diffraction efficiency of the +1st order was found to be 24%.

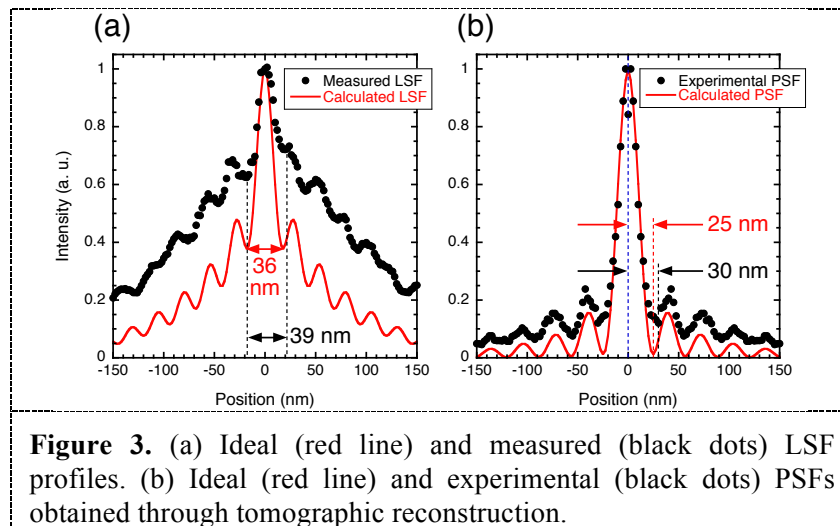


**Figure 3.** (a) Ideal (red line) and measured (black dots) LSF profiles. (b) Ideal (red line) and experimental (black dots) PSFs obtained through tomographic reconstruction.

### Acknowledgments

This work was supported by JSPS KAKENHI Grant Number 24510125. The synchrotron radiation experiments were performed at the BL24XU of SPring-8 with the approval of the Japan Synchrotron Radiation Research Institute (JASRI, Proposal Nos. 2014A3200, 2014A3203, 2014B3200 and 2014B3203). We would like to thank Editage ([www.editage.jp](http://www.editage.jp)) for English language editing.

### References

- [1] Yan H, Conley R, Bouet N and Chu Y S 2014 *J. Phys. D: Appl. Phys.* **47** 263001
- [2] Yamauchi K, Mimura H, Kimura T, Yumoto H, Handa S, Matsuyama S, Arima K, Sano Y, Yamamura K, Inagaki K *et al.* 2011 *J. Phys.: Condens. Matter* **23** 394206
- [3] Rehbein S, Heim S, Guttman P, Werner S and Schneider G 2009 *Phys. Rev. Lett.* **103** 110801
- [4] Vila-Comamala J, Jefimovs K, Raabe J, Pilvi T, Fink R. H, Senoner M, Maaßdorf A, Ritala M and David C 2009 *Ultramicroscopy* **109** 1360
- [5] Chao W, Kim J, Rekawa S, Fischer P and Anderson E. H. 2009 *Optics Express* **17** 17669
- [6] Rudolph D, Niemann B and Schmahl G *Proc. SPIE* 1982 **316** 103–5
- [7] Eberl C, Döring F, Liese T, Schlenkrich F, Roos B, Hahn M, Hoinkes T, Rauschenbeutel A, Osterhoff M, Salditt T *et al.* 2014 *Appl. Surf. Sci.* **307** 638–44
- [8] Keskinbora K, Robisch A-L, Mayer M, Sanli U T, Grévent C, Wolter C, Weigand M, Szeghalmi A, Knez M, Salditt T *et al.* 2014 *Opt. Express* **22** 18440–53
- [9] Koyama T, Takano H, Konishi S, Tsuji T, Takenaka H, Ichimaru S, Ohchi T and Kagoshima Y 2012 *Rev. Sci. Instrum.* **83** 013705
- [10] Takano H, Konishi S, Koyama T, Tsusaka Y, Ichimaru S, Ohchi T, Takenaka H and Kagoshima Y 2014 *J. Synchrotron Rad.* **21** 446–8
- [11] Hiroto T, Takano H, Sumida K, Koyama T, Konishi S, Ichimaru S, Ohchi T, Takenaka H, Tsusaka Y and Kagoshima Y 2016 *AIP Conference Proceedings* **1696** 020017
- [12] Takenaka H, Kawamura T, Ishii Y and Asagiri S 1995 *J. Appl. Phys.* **78** 5227–30
- [13] Schneider G 1997 *Appl. Phys. Lett.* **71** 2242–4
- [14] Maser J and Schmahl G 1992 *Opt. Commun.* **89** 355–62
- [15] Koyama T, Ichimaru S, Tsuji T, Takano H, Kagoshima Y, Ohchi T and Takenaka H 2008 *Appl. Phys. Express* **1** 117003
- [16] Yan H, Conley R, Bouet N and Chu Y S 2014 *J. Phys. D: Appl. Phys.* **47** 263001
- [17] Suzuki Y, Takeuchi A, Takano H and Takenaka H 2005 *Jpn. J. Appl. Phys.* **44** 1994–8